Statistical Copolymers with Side-Chain Hole and Electron Transport Groups for Single-Layer Electroluminescent Device Applications

Xuezhong Jiang[†] and Richard A. Register*

Department of Chemical Engineering, Princeton University, Princeton, New Jersey 08544

Kelly A. Killeen[‡] and Mark E. Thompson

Department of Chemistry, University of Southern California, Los Angeles, California 90089

Florian Pschenitzka and James C. Sturm

Department of Electrical Engineering, Princeton University, Princeton, New Jersey 08544

Received August 18, 1999. Revised Manuscript Received June 19, 2000

New statistical copolymers with bipolar carrier transport abilities were synthesized through free radical copolymerization of *N*-vinylcarbazole (NVK, hole-transport monomer) with either of two substituted styrenes containing oxadiazole groups, which serve as electron transport monomers: 2-phenyl-5-{4-[(4-vinylphenyl)methoxy]phenyl}-1,3,4-oxadiazole, PVO, and 2-(4-*tert*-butylphenyl)-5-{4-[(4-vinylphenyl)methoxy]phenyl}-1,3,4-oxadiazole, BVO. In all cases, the charge transport moieties exist in side groups, and carrier transport proceeds by hopping. Copolymerization yields homogeneous statistical copolymers of widely variable composition and thus tunable carrier transport properties; the copolymers are transparent in the visible region and form good films. Compared with systems where the oxadiazole units are incorporated by simply blending a small-molecule oxadiazole into poly(*N*-vinylcarbazole), the glass transition temperatures of these copolymers are high, and there is no possibility for the oxadiazole units to phase-separate through recrystallization. The glass transition temperatures for the copolymers show positive deviations from a harmonic mixing rule, suggesting some interaction between the NVK and BVO residues; however, blends of the homopolymers show limited miscibility at best, indicating that copolymerization is essential to produce a homogeneous material. Incorporating the oxadiazole units reduces the hole transport ability of these copolymers somewhat relative to NVK homopolymer, but single-layer dye-doped devices emitting blue, green, and orange light fabricated from these copolymers all showed good efficiency.

Introduction

Electroluminescence (EL) from small organic molecules[1] and polymers[2] forms the basis for their use in light-emitting diodes (LEDs). An LED produces light via the recombination of electrons and holes, injected from electrodes on opposite sides of the film. To achieve high luminescence efficiency, the electron and hole currents must be balanced, implying similar injection and transport behavior for the two types of carriers. However, typical organic molecules and polymers are not simultaneously good conductors for both electrons and holes. Heterostructured devices, where additional charge transport layers are inserted between the emission layer and the electrodes to facilitate charge injection and transport, are one means for improving device efficiency. Heterostructures also allow for insertion of hole- or electron-blocking layers adjacent to the emission layer to maximize recombination of carriers. However, multilayer devices are especially difficult to produce from polymers, as the layers are typically deposited by spin-coating, and only in unusual cases is it possible to choose a solvent that will dissolve the material being deposited and yet will not dissolve the previously deposited layers.[3−7] Another advantage of the single-layer device architecture is that the emitter can be incorporated in a patterned way after deposition of the carrier transport layer, such as via ink-jet printing of dye-containing solutions.[8]

* To whom correspondence should be addressed.
[†] Present address: Department of Materials Science and Engineering, Box 352120, University of Washington, Seattle, WA 98195.
[‡] Present address: Lexmark International Inc., 400 Circle Road NW, Lexington, KY 40550.

(1) Tang, C. W.; VanSlyke, S. A. *Appl. Phys. Lett.* **1987**, *51*, 913.
(2) Burroughes, J. H.; Bradley, D. D. C.; Brown, A. R.; Marks, R. N.; Mackey, K.; Friend, R. H.; Burns, P. L.; Holmes, A. B. *Nature* **1990**, *347*, 539.
(3) Greenham, N. C.; Moratti, S. C.; Bradley, D. D. C.; Friend, R. H.; Holmes, A. B. *Nature* **1993**, *365*, 628.
(4) Pommerehne, J.; Vestweber, H.; Guss, W.; Mahart, R. E.; Bässler, H.; Porsch, M.; Daub, J. *Adv. Mater.* **1995**, *7*, 551.
(5) Buchwald, E.; Meier, M.; Karg, S.; Pösch, P.; Schmidt, H. W.; Strohriegl, P.; Riess, W.; Schwoerer, M. *Adv. Mater.* **1995**, *7*, 839.
(6) Pei, Q.; Yang, Y. *Chem. Mater.* **1995**, *7*, 1568.
(7) Strukelj, M.; Papadimitrakopoulos, F.; Miller, T. M.; Rothberg, L. J. *Science* **1995**, *265*, 1969.

10.1021/cm990535v CCC: $19.00
Published on Web 07/26/2000

Another approach to improved efficiency retains the single-layer device structure but blends charge injection/transport molecules into a polymer matrix. A successful example[9,10] blends small-molecule oxadiazoles, which are good electron transporters, into poly(*N*-vinylcarbazole), PVK, a good hole transporter with a high glass transition temperature.[11,12] The electron-withdrawing character of the 1,3,4-oxadiazole ring in derivatives such as 2-(4-biphenyl)-5-(4-*tert*-butylphenyl)-1,3,4-oxadiazole, PBD,[9,10] facilitates electron injection and transport. Fabrication of such devices is straightforward, and good efficiencies and wide color tunability have been demonstrated.[9,10,13] The main concern with this approach is device stability: the level of added transport molecule is normally quite high, possibly leading to its phase separation by recrystallization and degraded device performance.[7] Polymers containing oxadiazole moieties in either the main chain[5,6] or a side group[7,14,15] have also been synthesized, but the hole-blocking nature of the oxadiazole group[16] makes such materials most useful as the electron transport or emissive layers in heterostructured devices. Simply blending such polymers with PVK in an attempt to balance the charge carrier density would likely lead to phase separation more severe than with the PVK:PBD blends.

Phase separation can be suppressed by covalently attaching the hole and electron transport moieties to the same polymer. Kido et al.[17] synthesized a strictly alternating copolymer of triarylamine (hole-transporting) and oxadiazole (electron-transporting) monomers, where the active groups were both present in the polymer backbone, and demonstrated this polymer's use in both undoped and dye-doped LEDs. Galvin and coworkers incorporated oxadiazole units into derivatives of poly(*p*-phenylenevinylene), PPV, either in the main chain[18,19] or in side groups.[20] Since the holes in PPV move through backbone conjugation, placing the oxadiazole units in the main chain (where they are in conjugation with the PPV units) produces a higher device efficiency.[19] However, even the PPV derivatives with oxadiazoles in the side chain showed greatly improved efficiencies, and related materials are still being developed.[21,22]

The closest analogue to the PVK:PBD blends would be a statistical ("random") copolymer prepared from *N*-vinylcarbazole and a monomer bearing a pendant oxadiazole unit. Unlike PPV, PVK transports holes through a hopping mechanism between the side-chain carbazole units,[23] so there should be little advantage to putting the oxadiazole units in the backbone. Statistical copolymerization (e.g., by a free-radical mechanism) offers a flexible and straightforward route to polymers having any desired composition, and thus tunable carrier transport properties, from two suitable monomers. However, such polymers have not been synthesized previously, possibly because of the difficulty in preparing monomers that will polymerize by a common mechanism and with comparable reactivity. Heischkel and Schmidt[24] produced block copolymers having PVK and oxadiazole blocks (the latter via post-polymerization grafting) via living cationic polymerization. Statistical copolymers would be difficult to generate by this approach, given the large differences in reactivities between monomers in ionic polymerizations.

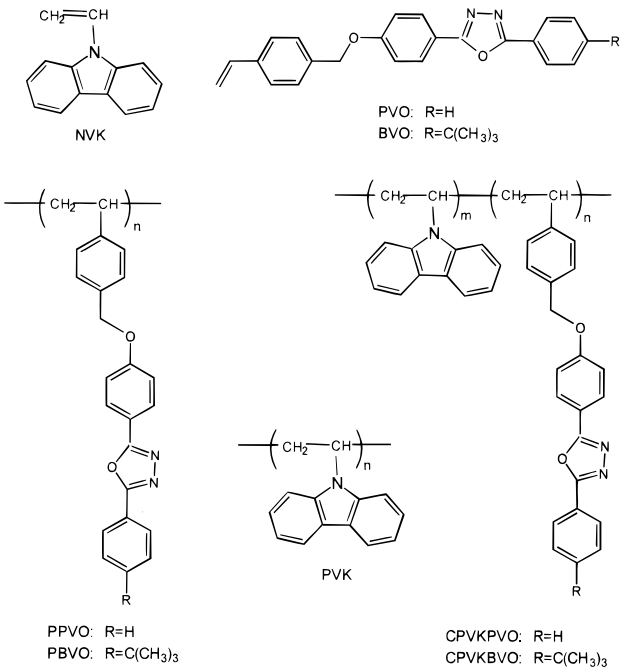

Figure 1. Structures of the monomers and polymers used in this work. The copolymers (CPVKPVO and CPVKBVO) are statistical copolymers; that is, the two monomer units shown are distributed essentially randomly along the chain.

Here, we report the synthesis of new copolymers (structures shown in Figure 1) that incorporate carbazole and oxadiazole groups through free radical copolymerization of *N*-vinylcarbazole, NVK, with two oxadiazole-bearing monomers: 2-phenyl-5-{4-[(4-vinylphenyl)-methoxy]phenyl}-1,3,4-oxadiazole, PVO, and 2-(4-*tert*-butylphenyl)-5-{4-[(4-vinylphenyl)methoxy]phenyl}-1,3,4-oxadiazole, BVO. The oxadiazole monomers are para-substituted styrenes; styrene and NVK copolymerize readily.[25]

Experimental Section

Monomer and Polymer Synthesis. Benzonitrile, 4-methoxybenzonitrile, 3-methoxybenzonitrile, *p*-anisoyl chloride,

(8) Hebner, T. R.; Sturm, J. C. *Appl. Phys. Lett.* **1998**, *73*, 1775.
(9) Kido, J.; Shionoya, H.; Nagai, K. *Appl. Phys. Lett.* **1995**, *67*, 2281.
(10) Wu, C. C.; Sturm, J. C.; Register, R. A.; Tian, J.; Dana, E. P.; Thompson, M. E. *IEEE Trans. Electron Devices* **1997**, *44*, 1269.
(11) Kido, J.; Hongawa, K.; Okuyama, K. *Appl. Phys. Lett.* **1993**, *63*, 2627.
(12) Jiang, X. Z.; Liu, Y. Q.; Song, X. Q.; Zhu, D. B. *Synth. Met.* **1997**, *87*, 175.
(13) Wu, C. C.; Sturm, J. C.; Register, R. A.; Thompson, M. E. *Appl. Phys. Lett.* **1996**, *69*, 3117.
(14) Cacialli, F.; Li, X.; Friend, R. H.; Moratti, S. C.; Holmes, A. B. *Synth. Met.* **1995**, *75*, 161.
(15) Li, X. C.; Cacialli, F.; Gilles, M.; Grüner, J.; Friend, R. H.; Holmes, A. B.; Moratti, S. C.; Yong, T. M. *Adv. Mater.* **1995**, *7*, 898.
(16) Brocks, G.; Tol, A. *J. Chem. Phys.* **1997**, *106*, 6418.
(17) Kido, J.; Harada, G.; Nagai, K. *Chem. Lett.* **1996**, 161.
(18) Peng, Z.; Bao, Z.; Galvin, M. E. *Adv. Mater.* **1998**, *10*, 680.
(19) Peng, Z.; Bao, Z.; Galvin, M. E. *Chem. Mater.* **1998**, *10*, 2086.
(20) Bao, Z.; Peng, Z.; Galvin, M. E.; Chandross, E. A. *Chem. Mater.* **1998**, *10*, 1201.
(21) Chung, S. J.; Kwon, K. Y.; Lee, S. W.; Jin, J. I.; Lee, C. H.; Lee, C. E.; Park, Y. *Adv. Mater.* **1998**, *10*, 1112.
(22) Chen, Z.-K.; Meng, H.; Lai, Y.-H.; Huang, W. *Macromolecules* **1999**, *32*, 4351.
(23) Pai, D. M. *J. Chem. Phys.* **1970**, *52*, 2285.
(24) Heischkel, Y.; Schmidt, H. W. *Macromol. Chem. Phys.* **1998**, *199*, 869.
(25) Hart, R. *Makromol. Chem.* **1961**, *47*, 143.

Scheme 1. Synthetic Route to PVO and BVO Monomers

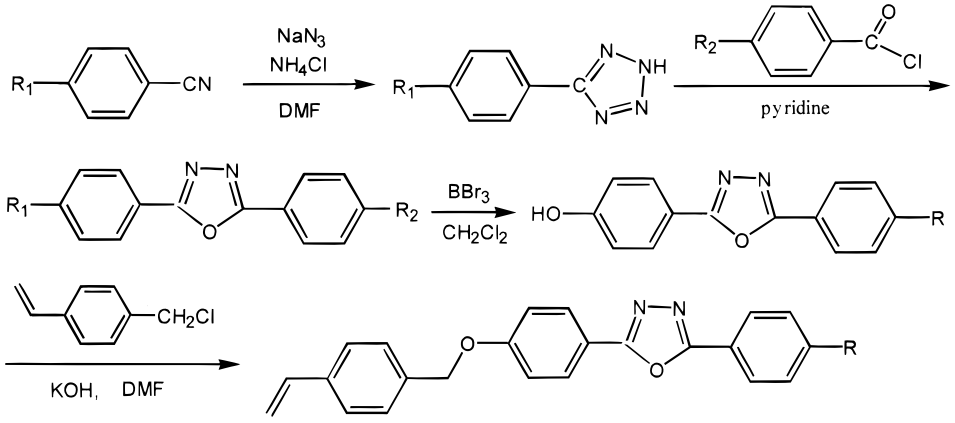

	R_1	R_2	R
PVO:	H	CH_3O	H
BVO:	CH_3O	$(CH_3)_3C$	$(CH_3)_3C$

4-*tert*-butylbenzoyl chloride, and 4-vinylbenzyl chloride (Aldrich) were used as received. NVK and azobis(isobutyronitrile), AIBN (Aldrich), were recrystallized from methanol twice before use. The synthetic route to PVO and BVO monomers is depicted in Scheme 1.

4-Methoxyphenyltetrazole:[26] A mixture of 4-methoxybenzonitrile (20.0 g, 150 mmol), sodium azide (14.65 g, 225 mmol), and ammonium chloride (12.05 g, 225 mmol) in *N*,*N*-dimethylformamide (DMF, 150 mL) was heated at 100 °C for 20 h. After cooling to room temperature the mixture was poured into 1.2 L of water and acidified with dilute HCl. The resulting white precipitate was collected, washed with water (4 × 100 mL), and dried in a vacuum at 60 °C. Yield: 18.58 g (70%). ^{1}H NMR ($CDCl_3$): 3.70 (s, 3 H); 7.11 (d, 2 H, $J_{HH} = 9$); 8.26 (d, 2 H, $J_{HH} = 9$); 14.7 (br, 1 H). MS $m/z = 176$ (M+).

Phenyltetrazole was prepared by refluxing benzonitrile (20.0 g, 194 mmol), sodium azide (18.91 g, 291 mmol), and ammonium chloride (15.56 g, 291 mmol) in DMF (150 mL). Yield: 25.21 g (90%). ^{1}H NMR (acetone-d_6): 7.58 (m, 3 H); 8.12 (dd, $J = 7$, $J = 3$, 2 H); 15.70 (br, 1 H).

2-(4-tert-Butylphenyl)-5-(4-methoxyphenyl)-1,3,4-oxadiazole:[26] 4-*tert*-Butylbenzoyl chloride (19.4 mL, 116 mmol) was added to a solution of 4-methoxyphenyltetrazole (18.50 g, 105 mmol) in pyridine (150 mL), and the mixture was refluxed for 2 h under argon. Water (300 mL) was added to the cooled reaction mixture affording a white precipitate. The precipitate was isolated, washed with water (3 × 100 mL), and dried in a vacuum at 60 °C. Yield: 31.03 g (96%). ^{1}H NMR ($CDCl_3$): 1.37 (s, 9 H); 3.89 (s, 3 H); 7.03 (d, 2 H, $J_{HH} = 9$); 7.54 (d, 2 H, $J_{HH} = 9$); 8.06 (t, 4 H, $J_{HH} = 9$).

2-(4-Methoxyphenyl)-5-(phenyl)-1,3,4-oxadiazole was prepared by the reaction of *p*-anisoyl chloride (12.84 g, 75.3 mmol) and phenyltetrazole (10.00 g, 68.4 mmol) in pyridine (100 mL). Yield: 15.96 g (92%). ^{1}H NMR (pyridine-d_5): 3.71 (s, 3 H); 7.11 (d, $J = 9$, 2 H); 7.49 (m, 3 H); 8.18 (d, $J = 9$, 4 H).

2-(4-tert-Butylphenyl)-5-(4-hydroxyphenyl)-1,3,4-oxadiazole: Boron tribromide (30.7 mL, 324 mmol) was vacuum transferred into a suspension of 2-(4-*tert*-butylphenyl)-5-(4-methoxyphenyl)-1,3,4-oxadiazole (20.0 g, 65 mmol) in CH_2Cl_2 (200 mL) at −196 °C. The reaction mixture was warmed to 0 °C and stirred under argon for 3 h and then quenched by the slow addition of Et_2O (75 mL) at 0 °C followed by addition of water (100 mL). The resulting white precipitate was isolated, washed with water (2 × 100 mL) and CH_2Cl_2 (3 × 100 mL), and then dried in a vacuum at 60 °C. The organic layer of the filtrate was separated and dried over $MgSO_4$. The solvent was removed in a vacuum, leaving pale peach solids which were combined with the original precipitate and extracted with a 2:1 mixture of acetone:pyridine (300 mL). The mixture was filtered, and water (300 mL) was added to precipitate the product from the filtrate. The white powder was collected, washed with water (3 × 100 mL), and dried in a vacuum at 60 °C. Yield: 13.40 g (70%). ^{1}H NMR (acetone-d_6): 1.36 (s, 9 H); 7.04 (d, 2 H, $J_{HH} = 9$); 7.64 (d, 2 H, $J_{HH} = 9$); 8.01 (d, 2 H, $J_{HH} = 8$); 8.06 (d, 2 H, $J_{HH} = 8$).

2-(4-Hydroxyphenyl)-5-(phenyl)-1,3,4-oxadiazole was prepared by the reaction of 2-(4-methoxyphenyl)-5-(phenyl)-1,3,4-oxadiazole (5.00 g, 19.8 mmol) and BBr_3 (18.7 mL, 198 mmol) in CH_2Cl_2 (100 mL). Yield: 2.93 g (62%). ^{1}H NMR (pyridine-d_5): 7.28 (d, $J = 9$, 2 H); 7.48 (m, 3 H); 8.19 (m, 4 H); 12.6 (br, 1 H).

2-(4-tert-Butylphenyl)-5-{4-[(4-vinylphenyl)methoxy]phenyl}-1,3,4-oxadiazole (BVO): Solid KOH (1.91 g, 34 mmol) was added to a solution of 2-(4-*tert*-butylphenyl)-5-(4-hydroxyphenyl)-1,3,4-oxadiazole (5.00 g, 17 mmol) and 4-vinylbenzyl chloride (5.18 g, 34 mmol) in DMF (75 mL), and the mixture was stirred for 6 h at room temperature. A colorless precipitate formed early in the bright yellow reaction mixture. Water (150 mL) was added to precipitate the product, which was isolated, washed with water (3 × 50 mL), and dried in a vacuum at 60 °C. Excess 4-vinylbenzyl chloride was removed by triturating the product in hexane (50 mL). The product was then washed with additional hexane (3 × 20 mL) and dried under a positive air flow. Yield: 6.72 g (96%). ^{1}H NMR ($CDCl_3$): 1.37 (s, 9 H); 5.14 (s, 2 H); 5.28 (d, 1 H, $J_{HH} = 11$); 5.78 (d, 1 H, $J_{HH} = 18$); 6.74 (dd, 1 H, $J_{HH} = 18$, $J_{HH} = 11$); 7.10 (d, 2 H, $J_{HH} = 9$); 7.43 (m, 4 H); 7.54 (d, 2 H, $J_{HH} = 9$); 8.05 (d, 2 H, $J_{HH} = 9$); 8.07 (d, 2 H, $J_{HH} = 9$). Melting point: 175 °C by DSC.

2-Phenyl-5-{4-[(4-vinylphenyl)methoxy]phenyl}-1,3,4-oxadiazole (PVO) was prepared by the reaction of KOH (0.94 g, 16.8 mmol), 2-(4-hydroxyphenyl)-5-(phenyl)-1,3,4-oxadiazole (2.00 g, 8.39 mmol), and 4-vinylbenzyl chloride (2.37 mL, 16.8 mmol) in DMF (50 mL). Yield: 2.97 g (100%). ^{1}H NMR ($CDCl_3$): 5.14 (s, 2 H); 5.28 (d, $J = 11$, 1 H); 5.78 (d, $J = 18$, 1 H); 6.74 (dd, $J = 18$, $J = 11$, 1 H); 7.10 (d, $J = 9$, 2 H); 7.50 (m, 7 H); 8.11 (m, 4 H).

Polymerization. Polymerizations were conducted in test tubes sealed with rubber septa, immersed in a water bath at 50 °C. Measured quantities of the solid NVK and PVO or BVO monomers and AIBN (0.03% w/w based on total monomer mass) were diluted to approximately 150 mg/mL in spectroscopic grade tetrahydrofuran (THF), and the solution was

(26) Bettenhausen, J.; Strohriegl, P. *Adv. Mater.* **1996**, *8*, 507.

deoxygenated by sparging with nitrogen for about 40 s. For the small-scale, low-conversion polymerizations used to determine radical reactivity ratios, the total monomer mass was about 50 mg, and the polymerizations were allowed to proceed for about 4 h (<10% conversion). The contents of the reaction mixture were then diluted to precisely 5 mL, and precisely 150 μL of the diluted solution was analyzed by gel permeation chromatography (GPC). The eluent from the GPC was collected and diluted as necessary for UV measurement, to determine both polymer composition and the conversion during polymerization. For the medium-scale polymerizations used to obtain material for DSC, 200 mg of monomer was used, and the polymerizations were allowed to run to about 20% conversion (15 h). For device fabrication, two large batches of polymer were made, using approximately 5 g of monomer and allowing the polymerizations to run to 30−40% conversion (about 25 h). The polymers were precipitated from THF into methanol at least twice, until the monomers were completely removed (as assessed by GPC). The polymers were then dried overnight at 50 °C in a vacuum. Homopolymerizations of PVK, PPVO, and PBVO were conducted similarly but at a higher concentration (about 300 mg/mL) and to higher conversions (2 days reaction time), as copolymer composition drift is not an issue.

Characterization. ^{1}H NMR spectra of the monomers and their precursors were recorded on a Bruker AC250 spectrometer. Chemical shifts are reported in ppm downfield from $SiMe_4$; coupling constants are reported in hertz. UV−vis spectra of the polymers were acquired using an HP 8452A diode array spectrometer. Molecular weights of the copolymers were determined by GPC in THF at 1.0 mL/min, using a Waters 590 pump, Polymer Laboratories 60 cm PLgel 5μ MIXED-C column, and Waters 490E programmable multiwavelength UV detector tuned to 254, 310, and 344 nm. Reported molecular weights are all relative to narrow-distribution polystyrene standards; weight-average molecular weights so determined were between 10 000 and 60 000 g/mol. Glass transition temperatures (T_g) were measured using a Perkin-Elmer DSC7 differential scanning calorimeter (DSC) at a scan rate of 10 °C/min, heating to at least 30 °C above the T_g. Indium, tin, and lead were used as calibration standards. Reported results for the copolymers were obtained on the second or third heat, and T_g values are taken at the half-height of the heat capacity step.

Device Fabrication and Testing. PBD, nile red (Aldrich), coumarin 6, and coumarin 47 (Lambda Physik) were used as received. ITO-on-glass substrates (Applied Films Corp., 25 Ω/□) were cleaned ultrasonically and treated with oxygen plasma, as described in detail elsewhere.[27] The polymer was deposited by spin-coating at 3500−4000 rpm from a 28 mg/mL solution in 1,2-dichloroethane in a nitrogen glovebox, producing films 700−1000 Å thick as measured by stylus profilometry. The copolymers have the good film-forming ability typical of high-molecular-weight glassy polymers; by low-voltage scanning electron microscopy, the films showed no cracks or pinholes down to 100 nm. A 1000 Å cathode layer of Mg:Ag (10:1) was evaporated at a pressure of 2×10^{-5} Torr to produce devices with active areas of 8 mm^2, followed by a 1000 Å cap layer of Ag. For "hole only" devices, Au was evaporated instead of the Mg:Ag and Ag layers. Devices employing PVK or PVK:PBD blends used the PVK synthesized as described above, rather than the commercial (cationically polymerized) PVK used in previous work.[10] Current−voltage and photocurrent−voltage characteristics were measured with a Hewlett-Packard 4145B semiconductor parameters analyzer and a calibrated Si photodiode system, all in a nitrogen atmosphere. EL spectra were recorded on a Photo Research PR-650 SpectraScan colorimeter. External quantum efficiencies are calculated as the measured photocurrent (from front-face emission only) divided by the device drive current, normalized for the photodiode assembly's known detection efficiency. Device brightnesses were obtained from the measured photodiode currents, using the relationship between photocurrent and brightness (measured on the PR-650) established for PVK:PBD blend devices[10] doped identically, as the EL spectra for both copolymer and blend devices are determined exclusively by the dye.

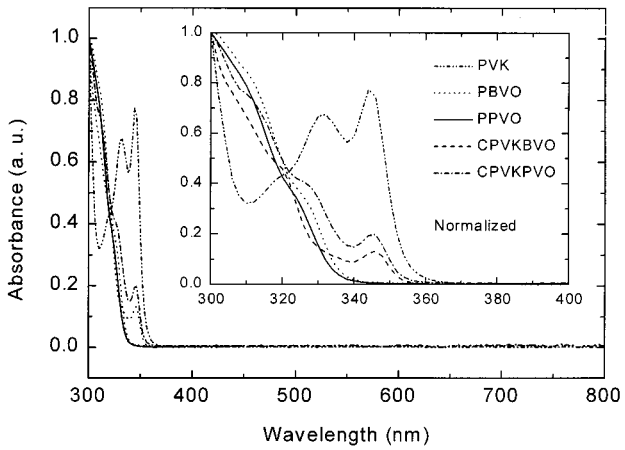

Figure 2. UV−vis spectra in THF of PVK, PBVO, and PPVO hompolymers, as well as an NVK/BVO copolymer (CPVKBVO, $F_1 = 0.66$) and an NVK/PVO copolymer (CPVKPVO, $F_1 = 0.55$). Inset shows the UV region on an expanded scale.

Results and Discussion

Figure 2 shows the UV−vis spectra of PVK, PPVO, and PBVO homopolymers and copolymers of NVK with BVO (CPVKBVO) and PVO (CPVKPVO). Neither the homopolymers nor the copolymers absorb significantly between 400 and 700 nm, meaning that these materials will not absorb the visible light from any emitter and should permit broad color tunability through the addition of appropriate emitter molecules (dyes). The copolymer compositions were determined from the UV absorbances of the copolymer at 310 and 345 nm, using the molar extinction coefficients ϵ (L/cm·mol repeat units) of PVK, PPVO, and PBVO homopolymers, which were measured as 1208, 22 070, and 25 960 at 310 nm and 2986, 111.2, and 124.6 at 345 nm, respectively. Throughout this paper, compositions will be expressed either as the mole fraction of NVK in the polymer (F_1) or as the weight fraction of NVK (w_1).

This method for composition determination implicitly assumes that the UV−vis spectra of the copolymers are simply the weighted averages of the UV−vis spectra of the homopolymers, an assumption confirmed for THF cosolutions of the homopolymers. For NVK/BVO copolymers, the spectra matched a linear combination of the homopolymer spectra to within 5% at any wavelength between 310 and 345 nm, so compositions determined in this fashion should be accurate to within 3%. However, more pronounced deviations (up to 50% at 328 nm) were observed for the NVK/PVO copolymers, making the composition determinations for these copolymers less certain. Unfortunately, the ^{1}H nuclear magnetic resonance spectra of all these polymers overlap extensively, and their C:H:N ratios are quite similar, meaning that neither ^{1}H NMR nor elemental analysis is a preferable assay.

Radical reactivity ratios were determined to permit the synthesis of polymers of well-controlled composition. For NVK and PVO, $r_{NVK} = 0.157 \pm 0.003$ and $r_{PVO} = 7.97 \pm 0.12$, while for NVK and BVO, $r_{NVK} = 0.066 \pm$

(27) Wu, C. C.; Wu, C. I.; Sturm, J. C.; Kahn, A. *Appl. Phys. Lett.* **1997**, *70*, 1348.

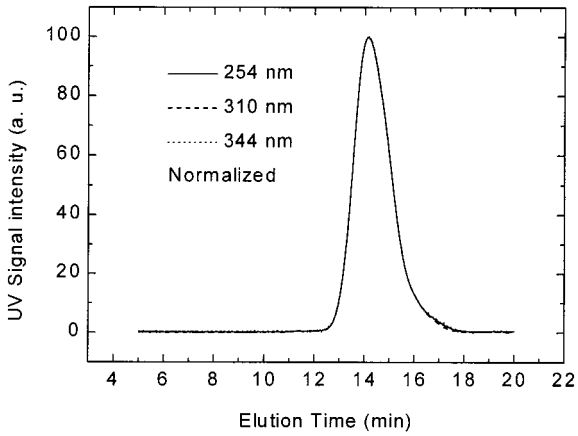

Figure 3. Chromatograms of a typical copolymer (NVK/BVO, $F_1 = 0.83$), recorded simultaneously at 254, 310, and 344 nm. Absorbances have been normalized to facilitate comparison of the three traces. This particular polymer was synthesized to relatively high conversion (30−40%; same polymer used in the devices reported on in Figures 9−11), yet the superposition of the chromatograms recorded at the different wavelengths indicates that the polymers are essentially homogeneous. Polystyrene-equivalent molecular weights derived from these chromatograms are $M_w = 60\,000$ g/mol and $M_n = 33\,000$ g/mol.

0.008 and $r_{BVO} = 12.4 \pm 1.0$. The quoted errors represent one standard deviation of the fit and do not include possible systematic deviations from the method of copolymer composition determination. The large difference in monomer reactivity causes a considerable drift in monomer composition during polymerization, meaning that conversion must be restricted to ensure a homogeneous copolymer. Fortunately, the more exotic BVO and PVO monomers are preferentially incorporated into the copolymer, so polymerizing to low total conversions is not impractical.

The homogeneity of the copolymers was assessed by GPC using multiwavelength detection. Chromatograms were recorded simultaneously at the standard 254 nm (detects aromatic nuclei on both monomer residues), at 310 nm (strong BVO and PVO absorption, modest PVK absorption) and at 344 nm (PVK peak absorption, little BVO or PVO absorption). Figure 3 shows a typical result: the chromatograms recorded at the three different wavelengths superimpose perfectly after normalization, confirming that the copolymers show no significant correlation between composition and molecular weight.

Since the active layers in LEDs may warm during device operation, materials having high glass transition temperatures are particularly desirable for enhancing the stability and lifetime of the devices.[7] Though PVK has a very high T_g (223 °C) when pure, blending large quantities of PBD into PVK can greatly suppress the T_g, increasing the likelihood that the PBD molecules can recrystallize. The T_g of PBD is 20 °C, measured on a partially amorphous specimen quenched in the DSC. Wu et al.[10] found that device efficiency was maximized at a blend ratio near 100:40 w/w PVK:PBD. Figure 4 shows DSC traces for a blend of PVK:PBD, prepared by codissolution in 1,2-dichloroethane (DCE) followed by solvent evaporation under flowing nitrogen. The PVK:PBD ratio here is approximately 100:40 w/w, though the gross phase separation which occurs during slow solvent evaporation makes it difficult to ensure

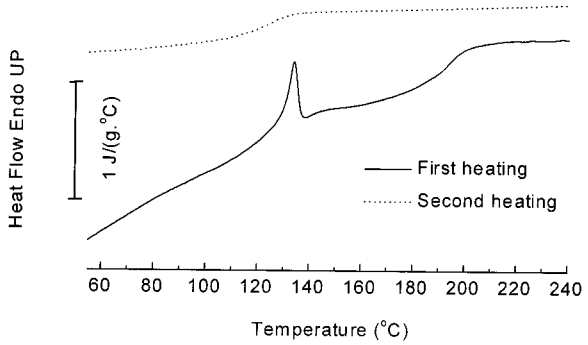

Figure 4. DSC traces of a PVK:PBD (approximately 100:40 by weight) blend, taken on the first heat (solid curve) and second heat (dashed curve).

Table 1. Characteristics of PVK and PBVO Homopolymers and Copolymers

polymer	PVK	KB1	KB2	KB3	KB4	PBVO
F_1	1	0.838	0.670	0.464	0.308	0
w_1	1	0.708	0.488	0.289	0.173	0
M_w (g/mol)	34000	28400	29700	21300	24300	21100
M_w/M_n[a]	2.02	1.41	1.63	1.43	1.45	1.87
T_g (°C)	223	203	185	166	157	140
ΔC_p (J/(g °C))	0.21	0.22	0.26	0.21	0.22	0.22

[a] The low polydispersities for the copolymers result from preferential removal of low-molecular-weight material during repeated precipitation. The higher polydispersities for the PVK and PBVO homopolymers result from the higher conversions employed in their syntheses.

Table 2. Performance Figures for Blend and Copolymer Devices (ITO/Polymer/Mg:Ag) Doped with 0.3 wt % Coumarin 6

polymer layer	turn-on voltage (V)	external quantum efficiency (%)
PVK:PBD (100:40 w/w)	13	0.45
CPVKBVO ($w_1 = 0.70$)	16	0.3

Table 3. Performance Figures for ITO/CPVKBVO/Mg:Ag Devices Doped with Different Dyes

dye	dye level (wt %)	turn-on voltage (V)	external quantum efficiency (%)	brightness (cd/m^2)[a]
coumarin 47 (blue)	0.65	9	0.10	8.4
coumarin 6 (green)	0.3	15	0.2	160
nile red (orange)	0.16	7	0.4	105

[a] Measured at 50 mA/cm^2 device current density (25 ± 2 V).

that the small DSC specimen has precisely this composition. The initial heating trace shows a sharp melting exotherm at 135 °C (the melting point, T_m, of PBD) and a glass transition at approximately 195 °C, indicating that much of the PBD crystallized out of the mixture during the sample preparation. The DSC scan taken on immediate reheat shows no melting exotherm and a single glass transition at 122 °C, indicating that the previously phase-separated PBD rapidly diffused into the PVK matrix to produce a homogeneous blend once the PVK T_g was exceeded.

By attaching the oxadiazole groups to the polymer backbone through copolymerization, the T_g penalty incurred in the blends can be largely avoided. The T_g values measured by DSC for the PPVO and PBVO homopolymers were 124 and 140 °C, respectively, vs 20 °C for the small-molecule PBD. Table 3 shows the molecular characteristics of NVK/BVO copolymers prepared to test this idea by DSC, for which traces are

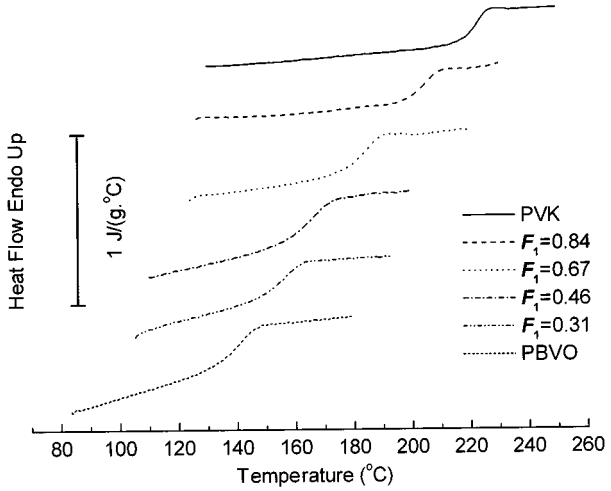

Figure 5. DSC traces for PVK, PBVO, and NVK/BVO copolymers spanning a range of compositions (mole fraction NVK indicated). Note the single sharp glass transition observed in all cases.

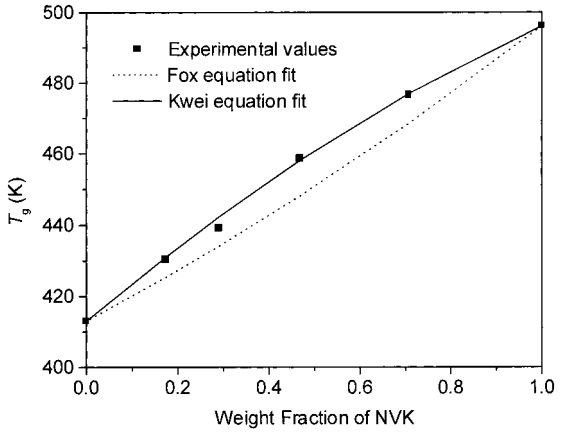

Figure 6. Variation of T_g with copolymer composition (weight fraction of NVK in copolymer) for NVK/BVO copolymers. Data are shown as solid squares; Fox equation as dashed line; best fit of the Kwei equation ($k = 1$, $q = 25$K) as solid line.

shown in Figure 5. The single glass transition and comparable heat capacity increment (ΔC_P) observed for all copolymers, along with the narrow transition widths, indicate that the copolymers are single-phase. Glass transition temperatures for copolymers without specific interactions between monomer residues are generally well-described by the Fox equation:[28]

$$\frac{1}{T_g} = \frac{w_1}{T_{g1}} + \frac{w_2}{T_{g2}} \qquad (1)$$

where w_i is the weight fraction of monomer i in the copolymer, and T_{gi} is the glass transition temperature (in absolute units) of the homopolymer of monomer i. Figure 6 compares the experimentally observed T_g values with the Fox equation prediction; the data show substantial positive deviations. The uncertainty in copolymer composition for the NVK/BVO copolymers is not more than 3%, so the deviations shown in Figure 6 are well outside experimental error. These positive deviations suggest that the NVK and BVO groups interact. The magnitude of this interaction can be

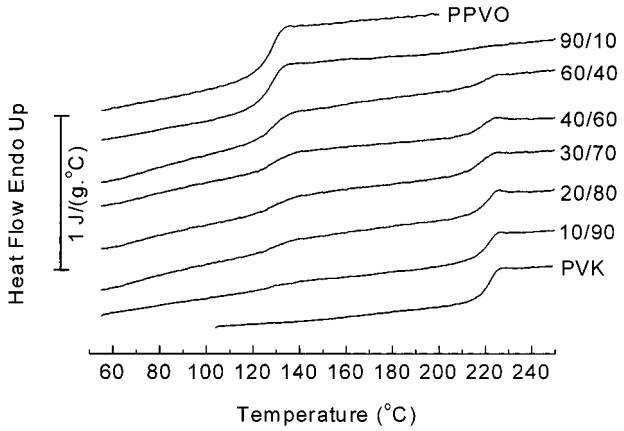

Figure 7. DSC traces for PVK ($M_w = 34$ kg/mol) and PPVO ($M_w = 10$ kg/mol) homopolymers and their blends at varying ratios (PVK:PPVO weight ratios indicated in figure).

quantified through the phenomenological Kwei equation:[29]

$$T_g = \frac{w_1 T_{g1} + k w_2 T_{g2}}{w_1 + k w_2} + q w_1 w_2 \qquad (2)$$

where k and q are system-specific parameters. This functional form provides a good fit to our data, as shown in Figure 6. The compositional uncertainties for the NVK/PVO copolymers are larger, precluding a meaningful comparison of the two systems.

If a positive specific interaction is indeed present, such as a charge-transfer complex between the carbazole and oxadiazole units, it might suffice to simply blend the carbazole- and oxadiazole-containing homopolymers, avoiding the need for copolymerization. Unfortunately, this turns out not to be so. Figures 7 (PVK:PPVO) and 8 (PVK:PBVO) show DSC curves for a series of homopolymer blends prepared at different weight ratios, casting from DCE under flowing nitrogen. At the composition midrange, two glass transitions are evident in both blend series, indicating that the polymers are not fully miscible. In the PVK:PPVO system, the transitions observed in the blends are at essentially the same temperatures as the transitions in the pure homopolymers, indicating complete immiscibility. By contrast, PVK and PBVO show some miscibility, as the transitions observed in the midrange of compositions are shifted inward relative to the T_g values of the homopolymers. Nonetheless, if a specific interaction exists here, it is too weak to compatibilize the blends; copolymerization is required to obtain homogeneous materials with broadly adjustable levels of hole and electron transport groups.

Devices fabricated from these copolymers are generally similar in performance to analogous PVK/PBD blend devices. Figure 9 shows the current−voltage and photocurrent−voltage curves for an orange device (doped with nile red, NR) having the configuration ITO/CPVK-BVO:nile red/Mg:Ag. In this case, the copolymer (NVK/BVO) had a composition $F_1 = 0.83$ ($w_1 = 0.70$), close to the optimum composition determined previously for PVK:PBD blend devices (100:40 w/w), and the nile red was added at 0.16 wt % of the polymer mass. The turn-

(28) Fox, T. G. *Bull. Am. Phys. Soc.* **1956**, *1*, 123.

(29) Kwei, T. K. *J. Polym. Sci., Polym. Lett. Ed.* **1984**, *22*, 307.

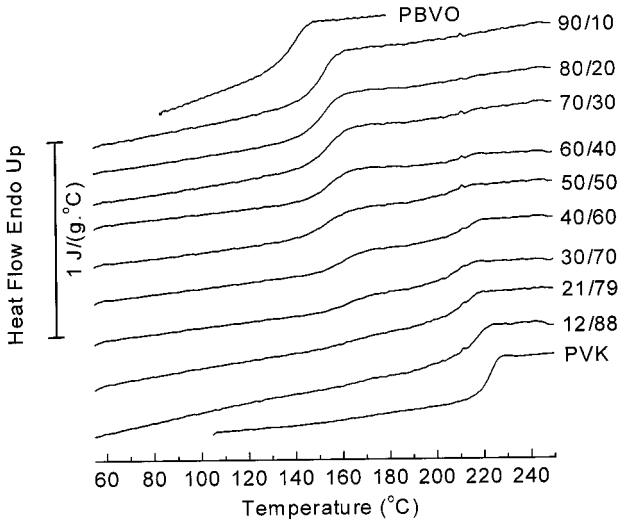

Figure 8. DSC traces for PVK (M_w = 34 kg/mol) and PBVO (M_w = 21 kg/mol) homopolymers and their blends at varying ratios (PVK:PBVO weight ratios indicated in figure).

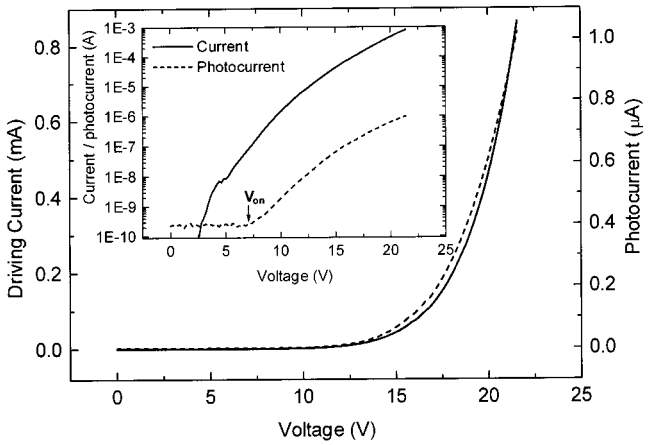

Figure 9. Current−voltage (solid) and photocurrent−voltage (dashed) characteristics of an ITO/CPVKBVO:nile red/Mg:Ag device (F_1 = 0.83; 0.16 wt % nile red dopant). Turn-on voltage is approximately 7 V.

on voltage, taken as the point where the photocurrent exceeds the dark current of the photodiode, is about 7 V. Table 2 compares performance figures for analogous blend and copolymer devices doped with coumarin 6 (C6, green). The copolymer device has a slightly higher turn-on voltage and lower efficiency than the blend device, but the two are comparable.

Figure 10 shows the electroluminescence spectra of orange, green, and blue devices prepared from the same copolymer by doping with different dyes. These EL spectra are identical to the photoluminescence spectra of the dyes themselves, indicating that device emission originates exclusively from the dyes. Table 3 provides performance figures for these devices, all fabricated in parallel (i.e., the C6 device is a different unit from that described in Table 2) and doped with dye at the same levels as analogous blend devices reported previously.[10] Device efficiencies are all on the order of 0.1%, with the orange device the most efficient and the blue device the least. This contrasts slightly with the PVK:PBD blend case,[10] where the green (C6-doped) device was the most efficient. Also, the turn-on voltage for the copolymer: C6 device is consistently higher than for devices made with the other two dopants, which is surprising if the

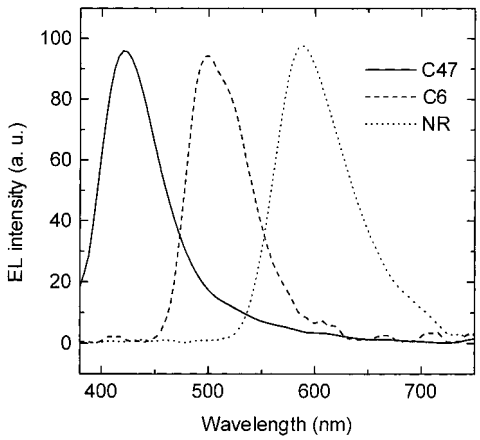

Figure 10. Electroluminescence (EL) spectra of ITO/CPVK-BVO/Mg:Ag devices (F_1 = 0.83) doped with coumarin 47 (C47, 0.65 wt %; blue device, solid curve), coumarin 6 (C6, 0.3 wt %; green device, dashed curve), and nile red (NR, 0.16 wt %; orange device, dotted curve).

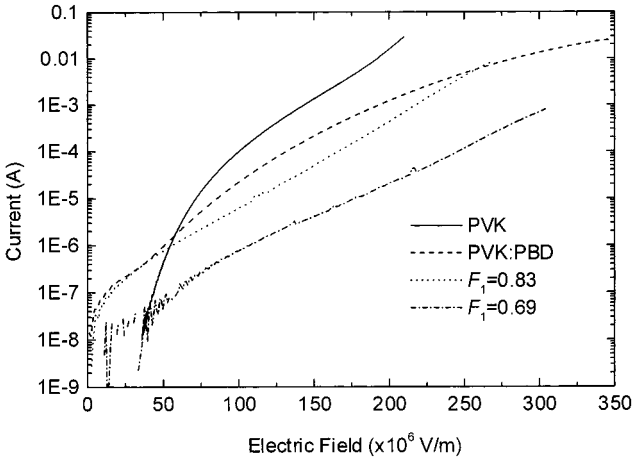

Figure 11. Current−voltage characteristics of undoped "hole only" devices, ITO/organic/Au. Compositions of the organic layers as indicated in figure; PVK:PBD 100:40 (w/w).

turn-on voltage is controlled by the hole injection ability of the matrix material (which is the same for all three devices). We are currently working to clarify this unexpected result. As with the PVK:PBD blend devices, the blue (C47) copolymer device is the least bright, achieving only 8 cd/m^2 at 50 mA/cm^2. By contrast, the green (C6) and red (NR) devices achieve brightnesses in excess of 100 cd/m^2 at this same device current, making them easily visible in a lit room.

To study how the oxadiazole groups modify the hole injection and transport ability of the copolymer, dye-free "hole only" devices were fabricated using Au as the cathode. Because the work function of Au is high, little electron injection should occur, and the magnitude of the driving current should reflect solely the hole injection and transport ability of the polymer film. Figure 11 shows the current−voltage characteristics (normalized for film thickness) of four devices, where the polymer layer is pure PVK, a PVK:PBD (100:40) blend, an NVK/BVO copolymer with F_1 = 0.83 (w_1 = 0.70), and an NVK/BVO copolymer with F_1 = 0.69 (w_1 = 0.51). At high operating voltages, the current decreases in precisely this order. Since the hole motion in these materials proceeds via irregular paths dictated by the locations of the hopping sites,[23] the "hole-blocking"[16] nature of the

oxadiazole groups, even if complete, would not prevent hole motion. However, note that the device fabricated from the copolymer with $F_1 = 0.83$ has a significantly lower hole current than the blend device over most of the voltage range, even though the concentration of carbazole and oxadiazole units in these two materials is quite similar. The higher current in the blend device may result from the regularity of the structure: since the carbazole units are strung together as a homopolymer, the next carbazole unit in a hopping path is never more than one repeat unit away. In the copolymer case, the hopping path between topologically adjacent carbazole units is frequently interrupted by the oxadiazole units.

Conclusions

We have synthesized new copolymers containing both hole and electron injection/transport groups through free radical copolymerization of *N*-vinylcarbazole (NVK) with 2-phenyl-5-{4-[(4-vinylphenyl)methoxy]phenyl}-1,3,4-oxadiazole (PVO) and 2-(4-*tert*-butylphenyl)-5-{4-[(4-vinylphenyl)methoxy]phenyl}-1,3,4-oxadiazole (BVO). The reactivity ratios of NVK and PVO were determined as $r_{NVK} = 0.157$ and $r_{PVO} = 7.97$, while those of NVK and BVO were $r_{NVK} = 0.066$ and $r_{BVO} = 12.4$; thus, the oxadiazole-containing monomer is depleted preferentially during copolymerization. The copolymers were homogeneous, as characterized by GPC (superposability of chromatograms taken at different UV wavelengths) and DSC (single narrow glass transition). The T_g values for the copolymers show significant positive deviations from the Fox equation but were well-correlated by the Kwei equation. Blends of the PVK and PPVO homopolymers were wholly immiscible, and PVK and PBVO showed only limited miscibility; to produce homogeneous materials where the carrier transport properties can be tuned over a wide range, copolymerization is essential. LEDs fabricated from these copolymers exhibited performance figures comparable to those for PVK blended with the small-molecule oxadiazole PBD, but without the possibility of recrystallization of the oxadiazole and degraded device performance. Single-layer dye-doped devices emitting blue (coumarin 47), green (coumarin 6), and orange (nile red) light fabricated from these copolymers all showed good efficiency. Measurements of hole current in "hole only" devices showed that the hole-blocking oxadiazole units do diminish the hole current relative not only to PVK homopolymer but also relative to analogous PVK:PBD blends, reflecting an interruption of the hole transport (hopping) path by the hole-blocking comonomer.

Acknowledgment. The authors acknowledge the generous financial support of the National Science Foundation, Optical Science and Engineering Program (ECS 96-12282), and the New Jersey Center for Optoelectronics, funded by the NJ Commission on Science & Technology. The authors are grateful for the experimental assistance of Neena Tierney (SEM) and Yichuan Huang (DSC of PBD).

Supporting Information Available: Tables of monomer feed, copolymer compositions, and molar conversions during polymerization in the small-scale NVK/PVO and NVK/BVO copolymerizations used for reactivity ratio determination. This material is available free of charge via the Internet at http://pubs.acs.org.

CM990535V